Supplementary Information - 1.

In this SI we shall comment on the similarity between pore connectivity values estimated by the dual-site-bond model (DSBM) and the standard method of Seaton. In ref [5] Armatas and Pomonis, compared the values of pore connectivity c in five (5) functionalized silicas, estimated by two methods: (i) The dual-site-bond model (DSBM) and Monte Carlo techniques for achieving the proper arrangement of the pores into the system and (ii) the standard method of Seaton. The comparison of the results obtained is in Plot I taken from Figure 8 of ref [5].

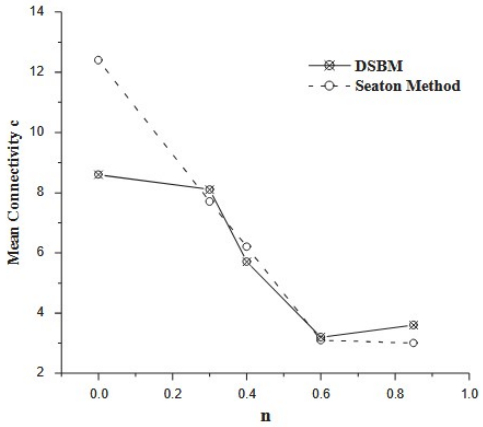

Plot I. Comparison of connectivity of functionalized silicas $SiO_2(STPI)_n$ as a function of n. STPI corresponds to silano-(trimethoxy)-propyl-imidazole group (from Figure 8 of ref [5]).

As can be seen, there is a very good matching between the two sets of values, except for sample n=0 (non-functionalized silica). Nevertheless, as mentioned in the present ms too, while the DSBM provides a distribution of connectivities, from which a mean connectivity (c_{mean}) is estimated, the method of Seaton leads to a singular average value ($c_{average}$). The peculiar point (somehow disregarded in ref [5]) is that the n=0 sample ehxibits two distinct ranges of connectivity disribution as shown in next Plot II, taken from Figure 9 of ref [5]. In that original Figure a single mean value of c was calculated (c=8.6) that is out of trend in Plot I.

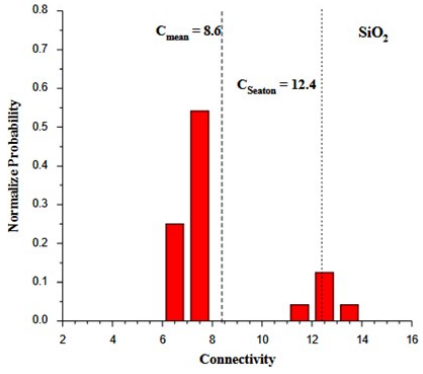

Plot II. The normalized to unity distribution of connectivity for sample SiO_2 (n=0). The c_{mean} and c_{Seaton} values are shown (from Figure 9 of ref [5].

Nevertheless if we estimate not a single but two different (c_{mean}) values for the two distinct distributions, we can easily obtain c(1,mean) ≈ 7 and c(2, mean) ≈ 13. This second value tallies impressively with the c_{Seaton} (= 12.4) in Plot I. This is also shown in next Plot III that exemplifies a very good linear relation between $c_{mean-\ DSBM}$ and $c_{average-Seaton}$ with correlation coeficient R^2 =0.997.

Sample $SiO_2(STPI)_n$	$c_{mean-\ DSBM}$	$c_{average-Seaton}$
n=0	13.0	12.4
n=0.30	8.1	7.7
n=0.40	5.7	6.2
n=0.60	3.2	3.1
n=0.85	3.6	3.0

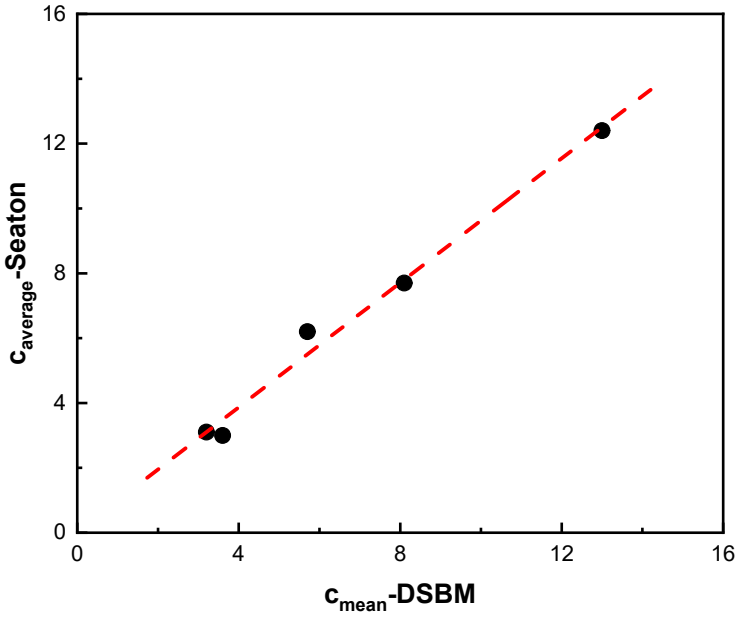

Plot III. The linear relation between $c_{mean-\ DSBM}$ and $c_{average-Seaton}$. The correlation coeficient for the relation $c_{average-Seaton}=0.96 \cdot c_{mean-\ DSBM}$ is $R^2=0.997$. All data from Figure 9 of ref [5] collected in the above Table.

So, the method of Seaton used in the present work, although not very analytical, provides meaningful and insightful results and in good agreement with the pore network based on the DSBM.

Supplementary Information - 2.

Nitrogen adsorption-desorption isotherms, e.g. $V_{N2\ ads} = f(P/P_0)$ and $V_{N2\ des} = f(P/P_0)$, of $Al_{100}P_XV_Y$ solids are shown in the left-bottom axes. The PSD's (dV/dD) (cc/g/nm) = f (D) (nm) are shown in the right-top axes. Notice the hyseresis loop observed between the adsortion and desortion branches. Data from refs [23,24]. Numerical values of pore characteristics of all materials are collected in the next Table S.I.-2.

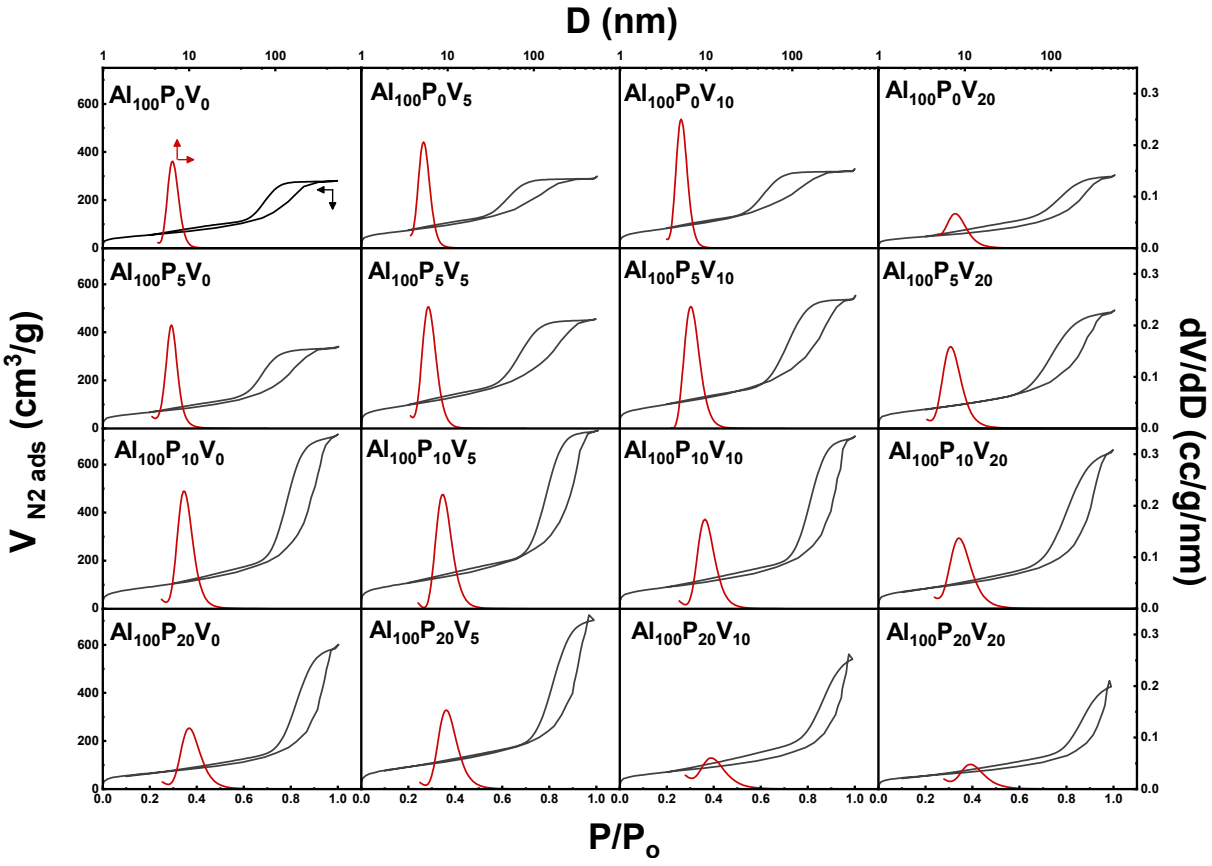

Table S.I.- 2. The sixteen (16) Alumino-Phosphoro-Vanadate materials $Al_{100}P_xV_y$ (x,y = 0, 5, 10, 20) and some of their properties. D_{max} is the pore diameter corresponding to the maximum of PSD's (dV/dD)= f (D) shown above. The Full Width at Half Maximum FWHM's of PSD's are also shown. Pore density N(pores/g) are also shown. Data from desorption branch of PSD and refs [23,24].

Sample	Pore connectivity $c_{average}$	Specific surface area S_p (m^2/g)	Specific Pore volume V_p (cm^3/g)	D_{max} of PSD (nm)	FWHM of PSD (nm)	[1] Pore number per g (N/g)= $[S^3]/[V^2]$)/ ($10^{12}/16\pi$)
$Al_{100}P_0V_0$	6.5	201.3	0.430	6.54	2.5	878,102
$Al_{100}P_5V_0$	12.3	245.3	0.518	*6.34*	*2.4*	1,094,923
$Al_{100}P_{10}V_0$	11.2	319.8	1.192	9.14	4.4	458,177
$Al_{100}P_{20}V_0$	14.0	239.5	0.928	10.74	6.3	317,520
$Al_{100}P_0V_5$	5.8	270.5	0.446	5.44	2.1	1,980,535
$Al_{100}P_5V_5$	7.0	352.6	0.703	6.24	2.9	1,765,577
$Al_{100}P_{10}V_5$	9.1	386.1	1.146	9.24	4.6	872,329
$Al_{100}P_{20}V_5$	9.6	336.0	0.475	10.34	5.9	3,346,424
$Al_{100}P_0V_{10}$	5.8	301.9	0.497	5.24	2.1	2,217,313
$Al_{100}P_5V_{10}$	7.8	359.0	0.833	6.94	3.4	1,327,222
$Al_{100}P_{10}V_{10}$	10.5	321.5	1.109	10.24	5.4	537,812
$Al_{100}P_{20}V_{10}$	15.0	257.9	0.358	12.44	10.2	2,664,025
$Al_{100}P_0V_{20}$	10.6	176.7	0.456	8.14	5.2	528,117
$Al_{100}P_5V_{20}$	9.0	286.3	0.743	7.34	4.1	846,129
$Al_{100}P_{10}V_{20}$	10.9	305.2	1.020	9.24	6.0	543,881
$Al_{100}P_{20}V_{20}$	15.2	199.9	0.245	12.64	10.3	2,648,845

[1] This parameter corresponds to the dimensioless ratio $[S^3]/[V^2]$ beween specific surface area S (m^2/g) and specific pore volumes V (cm^3/g). For details see P. Pomonis and A. Margellou, Phys Chem Chem Phys 19 (2017) 17441-17448

Supplementary Information – 3 .

The estimation of average pore connectivity $c_{average}$ for the 16 porous materials $Al_{100}P_XV_Y$, according to Seaton and co- workers [13-15], goes as follows: The bond occupation probability f is obtained as a function of percolation probability F from nitrogen adsorption-desorption isotherms using the pore size distribution and the following equations:

$$f = \frac{\int_{r^*}^{r=\infty} n_r \, dr}{\int_{0}^{r=\infty} n_r \, dr} \qquad \text{(S.I–2.1)}$$

$$\frac{f}{F} = \frac{V_{flat\ max} - V_{des}}{V_{flat\ max} - V_{ads}} \qquad \text{(S.I.-2.2)}$$

where n_r is the corresponding pore size distribution (psd) using the Barrett -Joyner - Halenda (BJH) method for cylindrical pores, $V_{flat\ max}$ is the part of desorption curve before the start of desorption, and V_{des} and V_{ads} are the corresponding volumes in the desorption and adsorption curves.

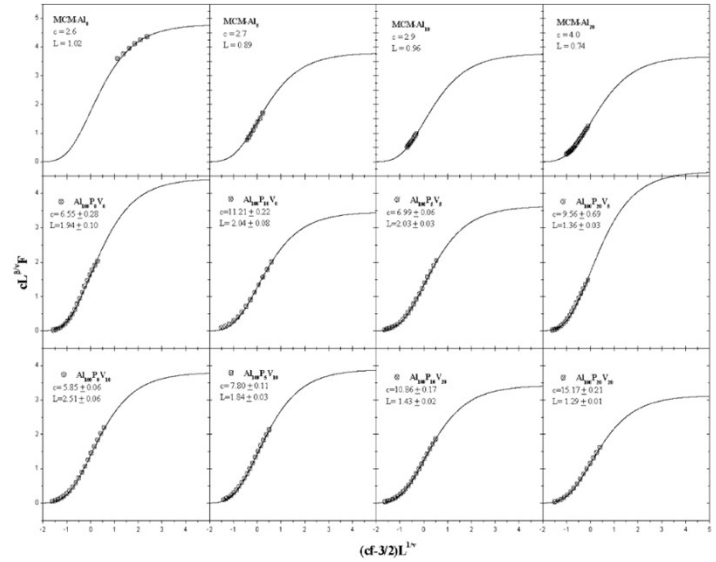

Figure S.I.-3. For the estimation of pore connectivity of materials $Al_{100}P_XV_Y$ plots of relation (S.I.–2.3) in the form $L^{\beta/\nu} F = g\,[cf- 3/2\ L^{1/\nu}]$ were employed. The fitting parameter c that corresponds to average connectivity as suggested by Kirkpatrick, S., In III-Condensed Matter.;

Ballian, R., Mayward, R., Toulouse, G., Eds.; North-Holland: Amsterdam, 1979. For more details see refs [23,24].

Then the best c (average connectivity) and L (a characteristic pore length parameter) values are obtained by fitting the experimental scaling data (F, f) to the scaling relation (S.I.- 2.3).

$$L^{\beta/\nu}\, cF = G\,[cf - 3/2\, L^{1/\nu}] \qquad \text{(S.I.–2.3)}$$

using the critical exponents $\beta = 0.41$ and $\nu = 0.88$. Typical fitting results of relation (S.I.–2.3) for the 16 porous materials $Al_{100}P_XV_Y$ used in this work , are repropduced next from refs [23,24].

Supplementary Information – 4 .

Table S.I.-4. Collective data of information entropy H (relation 1) and nanopore entropy E (relation 2) for samples $Al_{100}P_xV_y$. H(10), H(e) and H(2) are the H values from the PSD plots estimated according to relation (1), $H = -\sum_{1}^{n} pi\ log(pi)$ with logarithmic base b = 10 (units dits), e (units nats) and 2(units bits), respectively. Notation "H(10) (48-0.5) dits" means "H estimated with log base 10 using n = 48 p_i values with Bin Width = 0.5 nm and expressed in dits". E(10), E(e) and E(2) are the information entropy values H corrected according to relation (2) $E = e^H \bullet$ (Bin Width).

Sample	H(10) (48-0.5) (dits)	E(10)= $e^{H(10)}\bullet 0.5$ (nm)	H(e) (48-0.5) (nats)	E(e)= $e^{H(e)}\bullet 0.5$ (nm)	H(2) (48-0.5) (bits)	E(2)= $e^{H(2)}\bullet 0.5$ (nm)	H′(e) (24-1.0) (nats)	E′(e)= $e^{H'(e)}\bullet 1.0$ (nm)
$Al_{100}P_0V_0$	1.11	1.52	2.57	6.53	3.70	20.22	1.91	6.75
$Al_{100}P_5V_0$	1.15	1.58	2.64	7.01	3.81	22.58	1.98	7.24
$Al_{100}P_{10}V_0$	1.38	1.99	3.18	12.02	4.59	49.25	2.51	12.30
$Al_{100}P_{20}V_0$	1.52	2.29	3.51	16.72	5.06	78.80	2.83	16.95
$Al_{100}P_0V_5$	1.03	1.40	2.37	5.35	3.42	15.28	1.73	5.64
$Al_{100}P_5V_5$	1.16	1.59	2.66	7.15	3.84	23.26	2.01	7.46
$Al_{100}P_{10}V_5$	1.38	1.99	3.17	11.90	4.58	48.76	2.50	12.18
$Al_{100}P_{20}V_5$	1.50	2.24	3.44	15.59	4.97	72.01	2.77	15.96
$Al_{100}P_0V_{10}$	0.98	1.33	2.26	4.79	3.26	13.02	1.61	5.00
$Al_{100}P_5V_{10}$	1.22	1.69	2.80	8.22	4.04	28.41	2.14	8.50
$Al_{100}P_{10}V_{10}$	1.46	2.15	3.37	14.54	4.86	64.51	2.69	14.73
$Al_{100}P_{20}V_{10}$	1.63	2.55	3.74	21.05	5.40	110.70	3.06	21.33
$Al_{100}P_0V_{20}$	1.45	2.13	3.33	13.97	4.80	60.75	2.65	14.15
$Al_{100}P_5V_{20}$	1.36	1.95	3.14	11.55	4.53	46.38	2.46	11.70
$Al_{100}P_{10}V_{20}$	1.51	2.26	3.49	16.39	5.03	76.47	2.81	16.61
$Al_{100}P_{20}V_{20}$	1.63	2.55	3.75	21.26	5.41	111.82	3.08	21.76

Supplementary Information – 5 .

Figure S.I.-5. Variation of various expressions of information entropy H and nanopore entropy E as a function of pore connectivity c. ***Left:*** Information entropy H $= -\sum_{1}^{n} pi\ log(pi)$ (relation 1 in the text) estimated with different logarithmic bases b. *Top* → b=10, units dits; *Middle* → b=e, units nats; *Bottom* → b=2, units bits. Notation "H (10-48-0.5- dits)" means "Information entropy H estimated with log base b=10 using n= 48 pi values with Bin Width = 0.5nm and expressed in dits". ***Right:*** Nanopore entropy E = e^{H}• (Bin Width) (relation 2 in the text). Rest as in the right-hand-part. Notice that the data in the middle- left sub-figure, based on logarithmic base b = e, have been estimated for two different p_i values (n= 48 (●) and n=24 (▲)), the later providing lower H values as expected. This discrepancy has been eliminated in the middle- right sub-figure corrected by multiplying (exp H) with the corresponding Bin Widths 0.5 and 1.0 (nm).

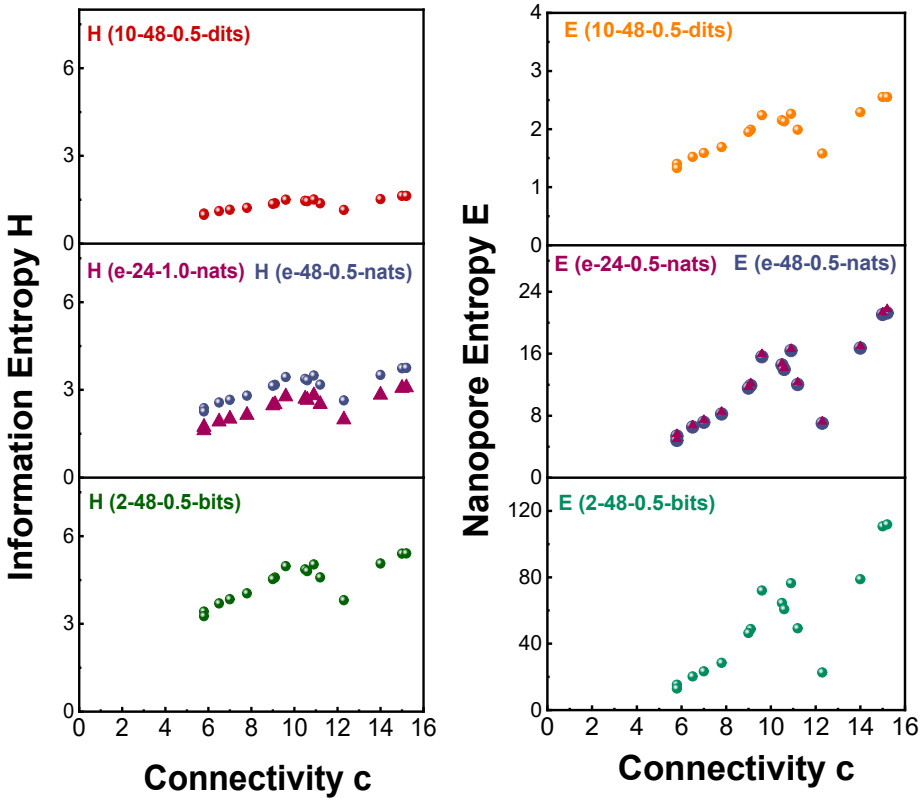

Supplementary Information – 6 .

Table S.I.-6. Logarithmic values of pore connectivity c, nanopore entropies E and information entropies H using logarithmic base b= 10 and e. Notations E(10) - H (10) , E(e)- H (e) and E(2) - H (2) indicate that the corresponding values have been estimated using decadic and natural and base respectively, according to the equations (1) and (2).

Sample	Conne-ctivity	$\log_{10}c$	$\log_e c$	E(10)	Log_{10} E(10)	H(10)= $\log_{10}$E(10) + 0.30	E(e)	Log_e E(e)	H(e)= $\log_e$E(e) +0.69
$Al_{100}P_0V_0$	6.5	0.81	1.87	1.52	0.18	0.48	6.53	1.88	2.57
$Al_{100}P_5V_0$	12.3	1.09	2.51	1.58	0.20	0.50	7.01	1.95	2.64
$Al_{100}P_{10}V_0$	11.2	1.05	2.42	1.99	0.30	0.60	12.02	2.49	3.18
$Al_{100}P_{20}V_0$	14.0	1.15	2.64	2.29	0.36	0.66	16.72	2.82	3.51
$Al_{100}P_0V_5$	5.8	0.76	1.76	1.40	0.15	0.45	5.35	1.68	2.37
$Al_{100}P_5V_5$	7.0	0.85	1.95	1.59	0.20	0.50	7.15	1.97	2.66
$Al_{100}P_{10}V_5$	9.1	0.96	2.21	1.99	0.30	0.60	11.90	2.48	3.17
$Al_{100}P_{20}V_5$	9.6	0.98	2.26	2.24	0.35	0.65	15.59	2.75	3.44
$Al_{100}P_0V_{10}$	5.8	0.76	1.76	1.33	0.12	0.42	4.79	1.57	2.26
$Al_{100}P_5V_{10}$	7.8	0.89	2.05	1.69	0.23	0.53	8.22	2.11	2.80
$Al_{100}P_{10}V_{10}$	10.5	1.02	2.35	2.15	0.33	0.63	14.54	2.68	3.37
$Al_{100}P_{20}V_{10}$	15.0	1.18	2.71	2.55	0.41	0.71	21.05	3.05	3.74
$Al_{100}P_0V_{20}$	10.6	1.03	2.36	2.13	0.33	0.63	13.97	2.64	3.33
$Al_{100}P_5V_{20}$	9.0	0.95	2.20	1.95	0.29	0.59	11.55	2.45	3.14
$Al_{100}P_{10}V_{20}$	10.9	1.04	2.39	2.26	0.35	0.65	16.39	2.80	3.49
$Al_{100}P_{20}V_{20}$	15.2	1.18	2.72	2.55	0.41	0.71	21.26	3.06	3.75

Supplementary Information – 7.

Table S.I.-7. Plots of data from Table S.-I.- 6. ***Left:*** Plots H(10) = -0.027+0.633·$\log_{10}$ c, (R^2 =0.921) and $\log_{10}$ E(10) = -0.327+0.634·$\log_{10}$ c (R^2=0.921). ***Middle:*** H(e)=-0.119+1.448·$\log_e$ c, (R^2=0.926) and $\log_e$ E(e) =-0.809+1.448·$\log_e$ c, (R^2=0.926). ***Right:*** $\log_2$ E(2) = -1.276 + 2.091·$\log_2$ c, (R^2= 0.924) and H(2) = -0.277+ 2.092·$\log_2$ c, (R^2= 0.924). This Figure is actually Figure 1 trans-scripted in log-log form. The vertical arrow corresponds to the $\log_b$(Bin Width) for b= 10, e, and 2. In all cases the out-of-trend point at right- middle has not been considered.

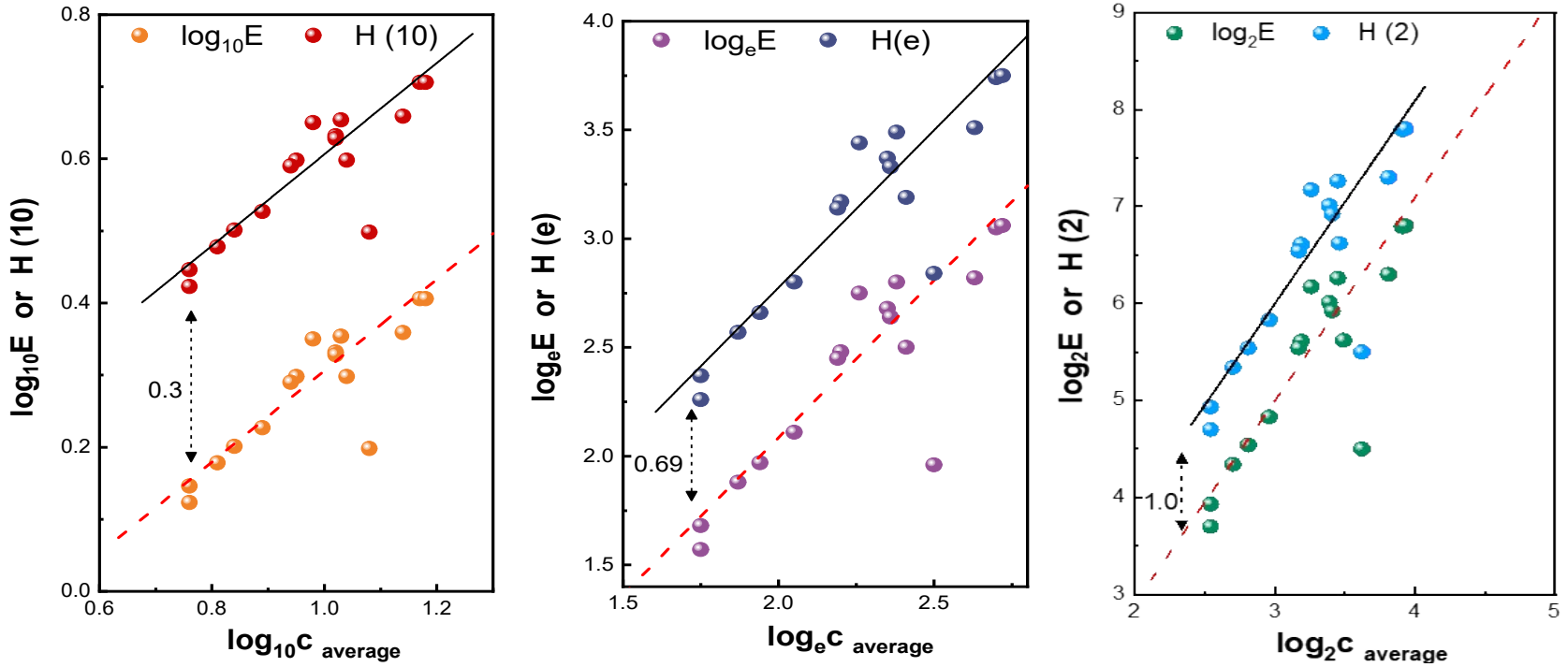

Supplementary Information – 8.

Table S.I.-8. Gaussian fitting results of experimental PSD's shown in S.I.-2 : x_c -position of curve maximum corresponding to D_{max} ; w-width of curve (2σ) corresponding closely to the full width at half maximum FWHM; A-area under the envelope of Gaussian curve; h-height of curve (maximum y) at x_c;; β- integral breadth, an alternative parameter to FWHM~2σ, defined as the ratio (peak area A/peak maximum h). This concept is common in characterization of peak shapes in XRD studies**.** R^2 – correlation coefficient of fitting the theoretical Gaussian to the experimental PSD's.

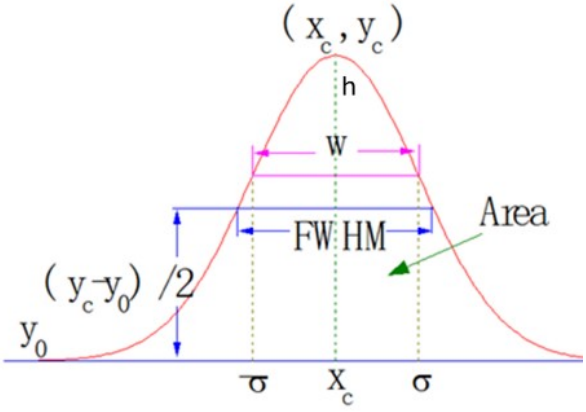

max

Sample	$x_c = D_{max}$	w	FWHM	A	h	β (A/h)	R^2
$Al_{100}P_0V_0$	6.566	1.859	2.189	0.391	0.168	2.327	0.982
$Al_{100}P_5V_0$	6.334	1.914	2.253	0.459	0.191	2.403	0.986
$Al_{100}P_{10}V_0$	9.143	3.352	3.947	0.956	0.228	4.193	0.960
$Al_{100}P_{20}V_0$	10.710	4.714	5.549	0.691	0.117	5.906	0.940
$Al_{100}P_0V_5$	5.382	1.623	1.911	0.411	0.202	2.035	0.986
$Al_{100}P_5V_5$	6.197	2.156	2.538	0.629	0.233	2.700	0.974
$Al_{100}P_{10}V_5$	9.235	3.444	4.055	0.976	0.226	4.319	0.948
$Al_{100}P_{20}V_5$	10.288	4.389	5.168	0.845	0.154	5.487	0.938
$Al_{100}P_0V_{10}$	5.259	1.525	1.796	0.475	0.248	1.915	0.983
$Al_{100}P_5V_{10}$	6.975	2.528	2.977	0.759	0.239	3.176	0.950
$Al_{100}P_{10}V_{10}$	10.246	4.067	4.788	0.885	0.174	5.086	0.948
$Al_{100}P_{20}V_{10}$	12.384	7.861	9.255	0.524	0.053	9.887	0.939
$Al_{100}P_0V_{20}$	8.143	4.484	5.279	0.348	0.062	5.613	0.977
$Al_{100}P_5V_{20}$	7.281	3.186	3.751	0.620	0.155	4.000	0.952
$Al_{100}P_{10}V_{20}$	9.214	4.499	5.297	0.742	0.132	5.621	0.944
$Al_{100}P_{20}V_{20}$	12.595	7.654	9.012	0.407	0.042	9.690	0.939